Inorganic Chemistry

Article

pubs.acs.org/IC

Cyclometalated Platinum Complexes with Luminescent Quantum Yields Approaching 100%

Eric Turner, Nathan Bakken, and Jian Li*

Materials Science and Engineering, Arizona State University, Tempe, Arizona 85287, United States

Supporting Information

ABSTRACT: A new class of cyclometalated tetradentate platinum complexes of the type Pt[N^\C−O−LL′] was synthesized and characterized. N^\C is a cyclometalating ligand such as phenyl-pyrazole (ppz), phenyl-methylimidazole (pmi), or phenyl-pyridine (ppy), and LL′ is an ancillary ligand such as phenoxyl-pyridine (popy). The complexes in this series are highly luminescent, emitting blue to green light in solution with quantum efficiencies ranging from 0.39 to 0.64 and luminescent lifetimes from 2 to 9 μs. When doped in a poly(methyl methacrylate) (PMMA) thin film, measured quantum efficiencies increase to 0.81−0.97 with lifetimes ranging from 4.5−10.4 μs. One notable example, the metal complex PtOO3, emits green light with a luminescent quantum efficiency approaching 100% and achieves approximately 100% electron-to-photon conversion efficiency in device settings.

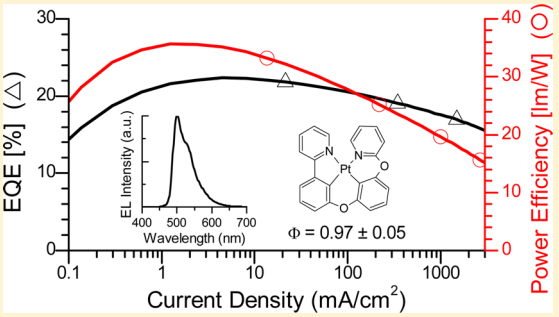

INTRODUCTION

Cyclometalated iridium and platinum complexes have been the focus of considerable research, driven in large part by their potential use as sensitizers,[1−3] photocatalysts,[4,5] and chemosensors.[6−8] These metal complexes have also attracted strong interest as luminescent materials for use in organic light emitting diode (OLED) based display and lighting applications[9−15] due to their ability to harvest both electro-generated singlet and triplet excitons, resulting in a theoretical 100% electron-to-photon conversion efficiency.[16,17] While both octahedral iridium complexes and square planar platinum complexes have rich histories in inorganic photophysics, iridium complexes have gained more prominence in OLED applications as their reported quantum yields have approached 100% and luminescent lifetimes have fallen into the microsecond range.[18] Despite the dominance of iridium at present, platinum remains an exciting field of study. If the intrinsic electroluminescent properties of phosphorescent platinum complexes can be unmasked and optimized, these complexes can provide a viable alternative to existing iridium emitters and spur further growth in this emerging field.

Square planar platinum complexes possess excellent structural flexibility, with the ability to employ various cyclometalating ligands. In doing so, the ground state and excited state properties of platinum complexes can be altered significantly.[19−21] Traditionally, those based on bidentate[22,23] and tridentate[24−29] ligands have been the most studied, but tetradentate complexes have seen expanded interest in recent years, with many highly efficient examples being reported. Tetradentate platinum complexes are attractive candidates for emitters due to their rigid framework which can aid in thermal stability, as well as reduce nonradiative decay pathways.[30]

A series of complexes have been developed by Che and coworkers that incorporate O^\N^\C^\N type ligands such as 5,5-dibutyl-2-(3-(pyridine-2-yl)-phenyl)-5H-indeno[1,2-*b*]pyridin-9-olate[31] and O^\N^\N^\O type ligands from Schiff bases such as *N*,*N*-bis(5-bromosalicylidene)-1,2-ethylenediamine[32] and bis(phenoxy)diimine based ligands such as 2,9-bis(2′-hydroxyphenyl)-4,7-diphenyl-1,10-phenanthroline.[33] Other notable examples include bis-cyclometalated complexes of the type N^\C*C^\N using ligands such as *N*,*N*-di(6-phenylpyridin-2-yl)aniline,[34] those of the type C^\N*N^\C using ligands such as *N*,*N*-di(3-(pyridine-2-yl)-phenyl)aniline[34] and 1,1-bis(6-(2,4-difluorophenyl)-2-pyridyl)-1-methoxyethane,[35] and those of the type C^\C*N^\N using ligands such as *N*,*N*-di((1,1′:3′,1″-terphenyl)-50-yl)-(2,20-bipyridin)-6-amine.[36] Several of these complexes have been incorporated into OLEDs, and while performance has been promising, it is still well below that of comparable iridium based emitters. To close the gap, judicious ligand design is needed to increase radiative decay rates while simultaneously restricting nonradiative decay mechanisms. Herein, we report the design, synthesis, and characterization of a series of highly emissive tetradentate, bis-cyclometalated platinum complexes that emit light in the blue to green region. Of note, a complex in this series based on phenyl-pyridine (ppy) has a luminescent quantum yield approaching 100%, a fast radiative decay process on a par with analogous iridium complexes, and approximately a 100% electron-to-photon conversion efficiency in an OLED.

Received: November 14, 2012

   dx.doi.org/10.1021/ic302490c | *Inorg. Chem.* XXXX, XXX, XXX−XXX

Scheme 1. Synthesis of Tetradentate Platinum Complexes of the Type N^C−O−LL′[a]

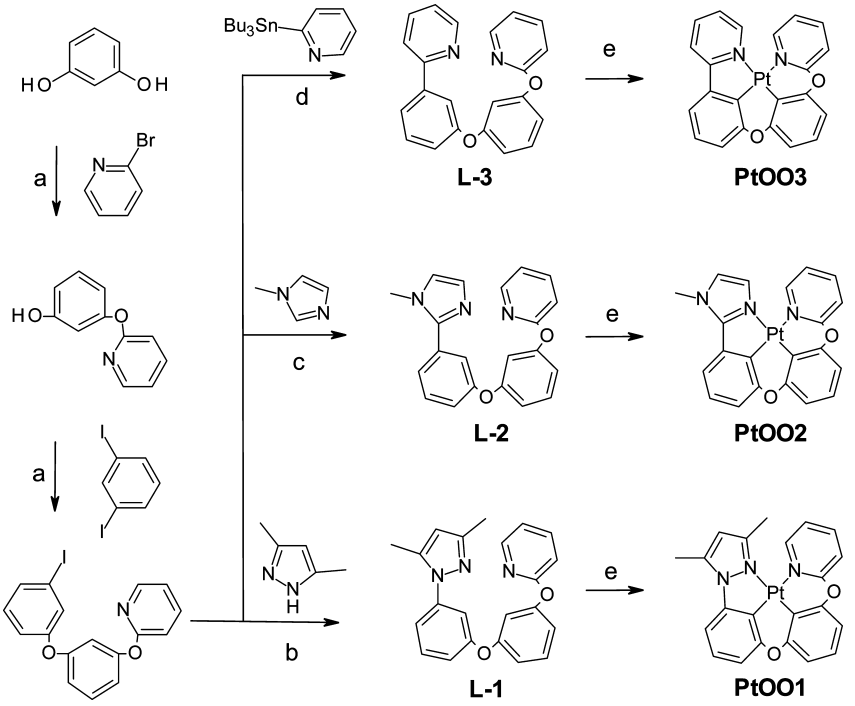

[a]Reagents and conditions: (a) 1-methylimidazole (0.5 equiv), K_2CO_3 (2 equiv), CuI (10%), pyridine/toluene (1:1), 120 °C. (b) Cu_2O (10%), syn-2-pyridinealdoxime (20%), Cs_2CO_3 (2.5 equiv), acetonitrile, reflux. (c) CuI (2 equiv), $Pd(OAc)_2$ (10%), 1-methylimidazole (1.5 equiv), DMF, microwave, 150 W, 160 °C. (d) tetrakis(triphenylphosphine)palladium(0) (5%), KF (1.2 equiv), toluene, reflux. (e) K_2PtCl_4 (1 equiv), AcOH, reflux.

RESULTS AND DISCUSSION

Design and Synthesis of Ligands and Complexes. The bulk of tetradentate complexes that have been reported recently fall into two main classes. Those reported by the Huo[34,36] and Marder[35] groups utilize symmetric ligands that incorporate a single six membered chelate ring containing a linking group such as nitrogen or carbon and an identical pair of five membered chelating rings built from units such as phenyl-pyridine or phenyl-pyrazole. In contrast, Che and co-workers have recently reported a diverse set of complexes that use aryl-phenolate groups, in both symmetric[33] and asymmetric[31] configurations, which incorporate varying numbers of five and six membered chelate rings. Given the design flexibility inherent in square planar systems, it is clear that the complexes that have been reported thus far represent only a small fraction of the set of possible designs.

When considering design criteria for new luminescent materials, the resulting complexes should remain rigid for the purposes of thermal stability and reduced nonradiative decay rates, be easily tunable to various emission energies, and have sufficiently fast radiative decay rates. A class of complexes was envisioned in which a portion of the ligand could be freely modified with widely reported cyclometalating motifs (N^C)[37] and coupled to a shared ancillary portion (LL′)[38] that would not directly contribute to the radiative decay process. This ancillary portion should be relatively easy to reduce and form an additional platinum−carbon bond to destabilize the well-known metal centered quenching states found in platinum complexes.[39] Phenoxyl pyridine (popy) was chosen to fill this role. The addition of the bridging oxygen between the (N^C) and popy portions enables facile metal coordination, whereas (N^C)Pt(popy) still remains as a synthetic challenge.

This design strategy results in a set of asymmetric tetradentate complexes of the type Pt[N^C−O−LL′]. To explore this class, three N^C motifs were selected: phenyl-pyrazole (ppz), phenyl-methylimidazole (pmi), and phenyl-pyridine (ppy). The N^C−O−popy ligands were prepared by two successive Williamson ether couplings[40] which were common to all three ligands, followed by a ligand specific final coupling. The first Williamson reaction produced the hydroxyl terminated phenoxypridine in modest yield. Special care was needed during the workup procedure to prevent deprotonation and decomposition of the intermediate product. The relatively poor solubility of HO−popy made recrystallization preferable to column chromatography for purification. The product of the second ether coupling was more robust, and the iodo-terminated intermediate was separated in good yield after column chromatography. The ligand ppz-O−popy (**L-1**) was prepared through an Ullmann-type reaction[41] with dimethyl-pyrazole, pmi-O−popy (**L-2**) through a palladium catalyzed C−C cross coupling microwave reaction[42] with 1-methylimidazole, and ppy-O−popy (**L-3**) through a Stille coupling[43] with 2-(tributylstannyl)pyridine. All ligands were purified through column chromatography. Detailed reaction and workup conditions are available in the Supporting Information. The Pt[N^C−O−LL′] complexes were prepared by direct metalation with K_2PtCl_4 in acetic acid. To achieve purity levels suitable for OLED devices, the crude products were purified by column chromatography, recrystallization, and train sublimation. These new platinum complexes were characterized by ^1H and ^{13}C NMR and CHN elemental analysis.

X-Ray Crystal Structure. Single crystals of PtOO1 were prepared by slow sublimation under high vacuum (10^{-6} Torr) conditions. The molecular structure deviates from square planar

dx.doi.org/10.1021/ic302490c | Inorg. Chem. XXXX, XXX, XXX−XXX

geometry due to the boat-like conformation of two six membered rings containing the oxygen linking atom, i.e., Pt1−C1−C−O1−C−C2 and Pt1−C2−C−O2−C−N3 (Figure 1), where the latter shows a larger degree of distortion. The

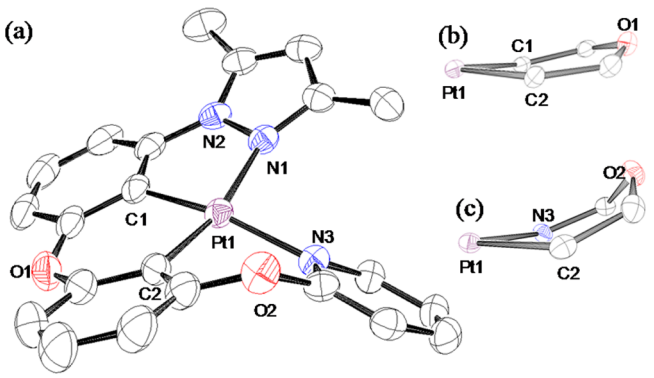

Figure 1. Perspective views of (a) PtOO1 with thermal ellipsoids representing the 25% probability limit, (b) the ring joining the two oxygen bridged phenyl rings, and (c) the ring joining the oxygen bridged phenyl and pyridyl rings. Hydrogen atoms were omitted for clarity.

existence of a bulky tetradentate ligand in the complex system also results in an increase of corresponding bond length. Compared with Pt(pzpyt)Cl,[44] where pzpyt is the ligand of 1-(1-pyrazolyl)-3-(2-pyridinyl)-toluene, the metal−ligand bond lengths in PtOO1 (Pt−$N1_{pz}$ = 2.097(3) Å, Pt−C1 = 1.970(4) Å, Pt−C2 =1.980(4) Å, and Pt−$N3_{py}$ = 2.093(3) Å) are significantly longer than their Pt(pzpyt)Cl counterparts (Pt−N_{pz} = 2.023(6) Å, Pt−C = 1.917(7) Å, and Pt−N_{py} = 2.040(6) Å).

Density Functional Theory. The calculated geometry of PtOO1 compares reasonably well with the one determined by X-ray crystallography, with both showing significant distortion from planarity of the popy ligand. The DFT generated metal−ligand bond lengths for Pt−$N1_{pz}$ (2.17 Å), Pt−C1 (2.00 Å), Pt−C2 (1.98 Å), and Pt−$N3_{py}$ (2.16 Å) are longer than those found in the crystal (Figure 1). The highest occupied molecular orbital (HOMO) and lowest unoccupied molecular orbital (LUMO) of the three tetradentate complexes are shown in Figure 2. In all reported compounds, the HOMO density is comprised of platinum metal, the oxygen bridging the two

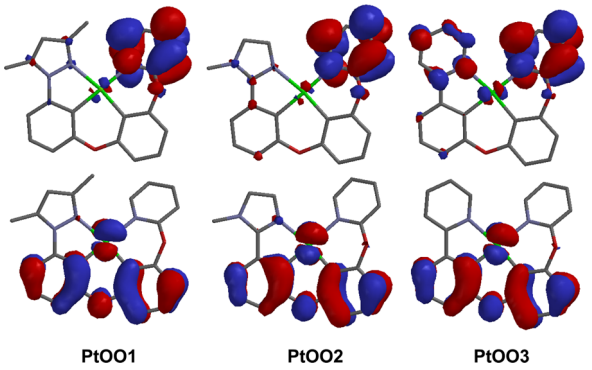

Figure 2. Highest occupied molecular orbital (HOMO) (bottom) and lowest unoccupied molecular orbital (LUMO) (top) of Pt[N^C−O−popy] complexes determined through density functional theory (DFT) calculations.

phenyl rings, and the two phenyl rings themselves, which is comparable to the distribution found in Pt[N^C−N−C^N] complexes using the ligands N,N-di(3-(3-methyl-1H-pyrazol-1-yl)phenyl)aniline and N,N-di(3-(pyridin-2-yl)-phenyl)aniline.[34] Of note, the oxygen bridge of the Pt[N^C−O−popy] complexes provides significantly less contribution to the HOMO than the triaryl amine in the comparable Pt[N^C−N−C^N] complexes. In the case of PtOO1 and PtOO2, the LUMO density is localized almost entirely on the pyridyl ring of the LL′ ligand, with minor contributions from the metal and the oxygen attached to the pyridyl ring. The LUMO density of PtOO3 has additional contribution from the (N^C) pyridyl ring.

Electrochemistry. The electrochemical properties of Pt[N^C−O−popy] complexes and analogs were examined using cyclic voltammetry and differential pulsed voltammetry. The electrochemical data (Table 1) reported here were measured relative to Fc/Fc^+. PtOO1, PtOO2, and PtOO3 all show an irreversible oxidation process typical of platinum complexes[45] between 0.33 and 0.62 V. Reduction occurs between −2.62 and −2.50 V. PtOO1 and PtOO2 both have levels of reversibility that are detectable only at scan speeds on the order of volts per second and are thus considered largely irreversible processes. In contrast, PtOO3 shows two well-defined quasi-reversible peaks at a scan speed of 100 mV/s (Figure S2). The reduction range of the tridentate complexes is significantly larger (−2.73 to −2.18 V) than their tetradentate analogues. This difference can be attributed to the fact that the pyrazolyl and imidazoyl groups in the tridentate complexes are more difficult to reduce than the pyridyl groups in PtOO1 and PtOO2, indicating that the first reduction process of the latter occurs primarily on the pyridyl group from the popy ligand. This is supported by the LUMO assignment calculated with density functional theory (Figure 2), which is composed mainly of this pyridyl ring.

Photophysical Properties. The emission spectra in solution at room and cryogenic (77 K) temperatures and in a doped PMMA film were recorded for all three Pt[N^C−O−popy] complexes along with their Pt(N^C^N)Cl and ppy analogs (Table 1). The absorption features of PtOO1, PtOO2, and PtOO3 are largely similar (Figure 3) with $^1\pi-\pi^*$ ligand centered (LC) transitions occurring below 300 nm, metal-to-ligand charge transfer (MLCT) transitions in the 300−420 nm range, and weaker, broad triplet transitions occurring near the energy of maximum emission at 77 K (Figure 4).

At 77 K, PtOO1, PtOO2, and PtOO3 show sharp vibronic progressions of 1380 cm^{-1}, 1440 cm^{-1}, and 1380 cm^{-1}, respectively, which is typical of complexes emitting from a predominantly ligand centered triplet state. The emission energy of PtOO1, PtOO2, and PtOO3 is strongly dependent on the reducibility of the N contributing aryl ring of the N^C ligand, with emission maxima ranging from 420 to 487 nm.

At room temperature, the synthesized Pt[N^C−O−popy] compounds are highly luminescent in degassed dichloromethane solution, emitting light in the blue to green region of the spectrum (Figure 5). The vibronic progressions of PtOO1 and PtOO3 become poorly resolved at this temperature, while those of PtOO2 are comparatively intact. Quantum efficiencies in solution range from 0.39 to 0.64 and in thin film from 0.81 to 0.97, which is among the highest reported for platinum based emitters. In the case of PtOO1, it far exceeds the comparable iridium compound *fac*-Ir(ppz)$_3$ ($\Phi < 0.01$),[18] as well as the analogous tridentate Pt(dpzb)Cl (Φ<0.01, Table 1). Furthermore, it emits at significantly higher energy than

dx.doi.org/10.1021/ic302490c | Inorg. Chem. XXXX, XXX, XXX−XXX

Table 1. Photophysical and Electrochemical Properties of Pt[N^C−O−popy] Complexes and Their Analogs

	emission at RT[a]					emission at 77K[b]			
	λ_{max} [nm]	Φ[c]	τ [μs]	k_r[d] [x10^5 s^{-1}]	k_{nr}[d] [x10^5 s^{-1}]	λ_{max} [nm]	τ [μs]	E_{ox}[e] [V]	E_{red}[e] [V]
PtOO1	430, 456	0.39 (0.83)	3.0 (7.5)	1.3 (1.1)	2.0 (0.23)	420	13	0.62	−2.59
Pt(dpzb)Cl[29]	432	<0.01 (0.02)	<0.1 (0.7)	(~0.3)	>100 (14.8)	426	14	0.57	−2.72
PtOO2	468	0.64 (0.81)	9.0 (10.4)	0.71 (0.78)	0.40 (0.18)	462	12	0.33	−2.62
Pt(dmib)Cl[29]	470	0.56	11	0.51	0.40	465	12	0.31	−2.73
PtOO3	512	0.63 (0.97)	2.0 (4.5)	3.2 (2.2)	1.8 (0.07)	487	4.9	0.38	−2.50
Pt(dpyb)Cl[24]	490	0.60 (0.73)	3.8 (5.7)	1.6 (1.3)	1.1 (0.47)	487	7.2	0.41	−2.18
(ppy)Pt(acac)[22]	484	0.15 (0.53)	2.6 (6.0)	0.58 (0.88)	3.3 (0.78)	480	9.0	0.42	−2.41

[a]Room temperature emission spectra were measured in a solution of dichloromethane or in a doped PMMA film (in parentheses). [b]The 77 K emission spectra were measured in a solution of 2-MeTHF. [c]Coumarin 47 was used as a reference for quantum efficiency measurement in a dilute solution. [d]The radiative decay rate (k_r) and the nonradiative decay rate (k_{nr}) are calculated based on the quantum efficiency and luminescent lifetime of samples in a dilute solution or a doped PMMA film (in parentheses). [e]Redox measurements were carried out in anhydrous DMF solution using DPV. The redox values are reported relative to Fc/Fc$^+$.

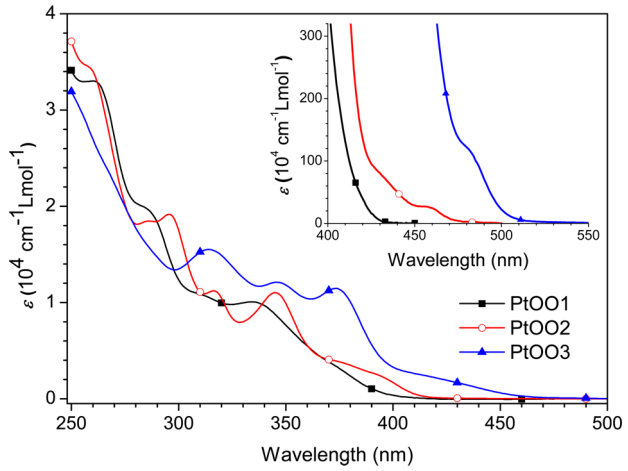

Figure 3. The comparison of the absorption spectra of PtOO1, PtOO2, and PtOO3 in CH_2Cl_2 at room temperature. The T_1 absorption transitions are shown in the inset.

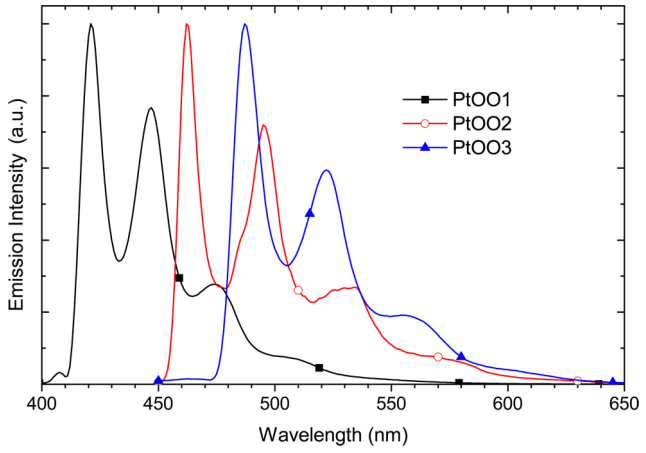

Figure 4. The 77 K emission spectra of PtOO1, PtOO2, and PtOO3 in 2-methyltetrahydrofuran.

efficient platinum complexes based on *N*,*N*-di(3-(1*H*-pyrazol-1-yl)phenyl)aniline ligands.[34] Interestingly, unlike several other reported tetradentate platinum complexes,[31,33,34] no excimer based emission was observed regardless of concentration for any of the presented compounds. This is likely due to the considerable distortion from planarity induced by the oxygen

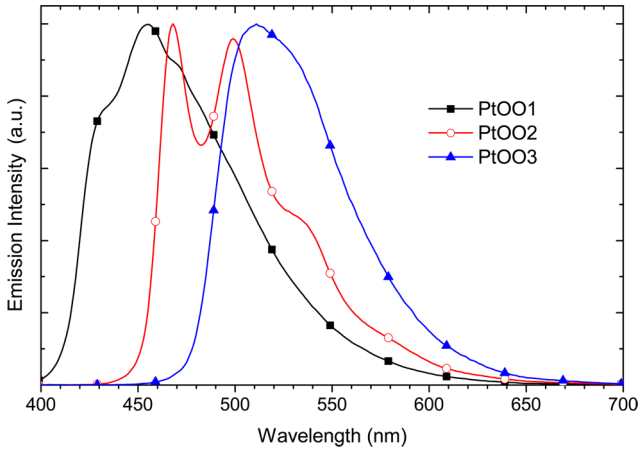

Figure 5. Room temperature emission spectra of PtOO1, PtOO2, and PtOO3 in dichloromethane.

linking atoms, which inhibits the intermolecular interactions necessary for excimer formation.

Study of PtOO3 and its Analogues. In order to better understand the influence of the (popy) ligand on the photophysical properties of platinum complexes, a series of ppy-based cyclometalated metal complexes were synthesized and characterized for comparison (Figure 6). This included the bidentate complex (ppy)Pt(acac),[22] the tridentate complex Pt(dpyb)Cl,[24] where dpyb is dipyridylbenzene, and the tris-cyclometalated complex *fac*-Ir(ppy)$_3$.[17]

All three (ppy)Pt-based complexes have an irreversible oxidation process but a quasi-reversible reduction process. The reduction potential of PtOO3 is similar to that of (ppy)Pt(acac), which is about 300 mV more negative than that of Pt(dpyb)Cl. This can be attributed to the influence of extending conjugation from ppy to the dpyb ligand. A similar trend was observed when other (C^N)Pt(acac) complexes were compared to their Pt(N^C^N)Cl analogs.[25]

A comparison of absorption features among PtOO3, Pt(dpyb)Cl, (ppy)Pt(acac), and *fac*-Ir(ppy)$_3$ complexes is shown in Figure 7. The platinum and iridium complexes exhibit very strong absorption bands below 300 nm due to $^1\pi-\pi^*$ ligand centered (LC) transitions, together with a set of intense bands in the region 300−420 nm, which is attributed to MLCT transitions involving both ligands and metal ions. The weak absorption bands between 470 and 500 nm can be identified as a triplet transition ($S_0 \rightarrow T_1$) on the basis of the

dx.doi.org/10.1021/ic302490c | Inorg. Chem. XXXX, XXX, XXX−XXX

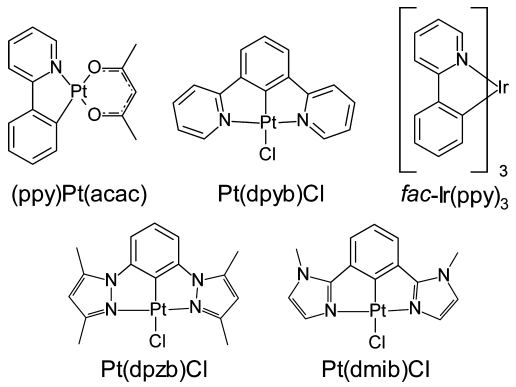

Figure 6. Structures of the synthesized ppy based comparative complexes (top) and the structures of literature reported ppz and pmi based comparative N^C^N tridentate complexes (bottom) discussed in this paper.

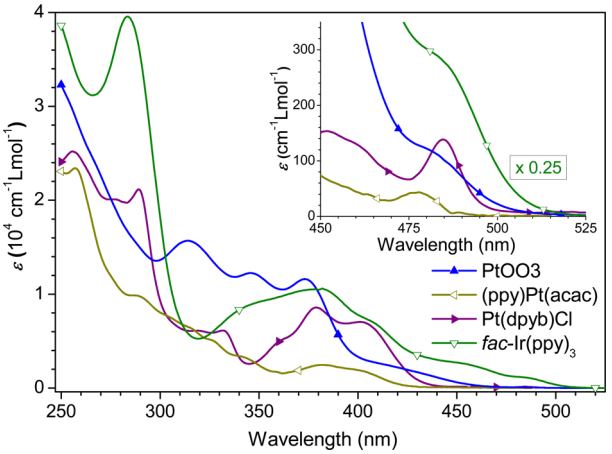

Figure 7. The comparison of the absorption spectra of PtOO3, Pt(dpyb)Cl, (ppy)Pt(acac), and *fac*-Ir(ppy)$_3$ complexes in CH_2Cl_2 at room temperature. The T_1 absorption transitions are shown in the inset.

small energy shift between absorption and emission at room temperature. PtOO3 possesses similar absorption features to Pt(dpyb)Cl and (ppy)Pt(acac) for LC and MLCT transitions in the range of 350−420 nm. The T_1 absorption of PtOO3 has fewer features and is more intense (based on integration area) than its platinum analogues, but weaker than *fac*-Ir(ppy)$_3$.

All three ppy based platinum complexes are strongly luminescent with quantum yields (Φ) ranging between 0.15 and 0.63 in solution and 0.53 and 0.97 in a doped PMMA film. All have luminescence lifetimes (τ) at room temperature which fall between 2 and 9 μs in solution and 4 and 10 μs in a PMMA film. The emission spectra of PtOO3, Pt(dpyb)Cl, (ppy)Pt(acac), and *fac*-Ir(ppy)$_3$ complexes at room temperature are shown in Figure 8. While both Pt(dpyb)Cl and (ppy)Pt(acac) possess structured luminescent spectra with well resolved vibronic progressions, the spectrum of PtOO3 is significantly less resolved, similar to that of *fac*-Ir(ppy)$_3$. Moreover, when compared to its platinum analogues, PtOO3 demonstrates a shorter luminescent lifetime (around 2 μs), a higher quantum yield (0.63), and a larger rigidochromic shift between room temperature and 77 K.[48] Similar to *fac*-Ir(ppy)$_3$,[17] PtOO3 has a measured emission quantum yield in doped PMMA film that approaches 100%. Taking this thin film data into account, the quantum yield of PtOO3 compares favorably with the currently

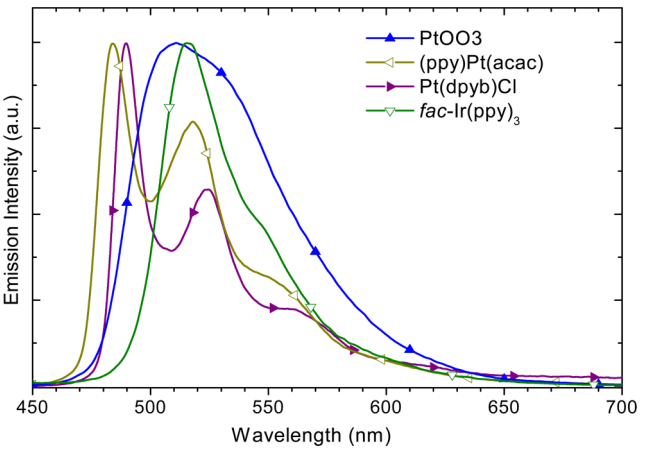

Figure 8. The emission spectra of PtOO3, Pt(dpyb)Cl, (ppy)Pt(acac), and *fac*-Ir(ppy)$_3$ complexes in CH_2Cl_2 at room temperature.

reported tetradentate homoleptic bis-cyclometalated platinum complexes [1,1-bis(6-(4,6-difluorophenyl)-2-pyridyl-N,C2)-1-methoxyethane]-platinum(II) (Φ = 0.54, τ = 0.38 μs)[35] and the highly efficient [N,N-di(2-phenylpyrid-6-yl)aniline]-platinum(II) (Φ = 0.74, τ = 7.6 μs)[34] while possessing a shorter lifetime than the latter. All comparisons indicate that the use of the (popy) ligand favorably alters the ground and excited state properties of platinum complexes, making them comparable to the state-of-the-art cyclometalated iridium complexes.

OLED Application. Devices employing PtOO3 as an emitter were compared with *fac*-Ir(ppy)$_3$ in the device structure: ITO/PEDOT:PSS/20 nm TAPC/25 nm 26mCPy:emitters(8%)/10 nm PO15/30 nm BmPyPB/LiF/Al. As shown in Figure 9, both devices exhibit external quantum efficiencies

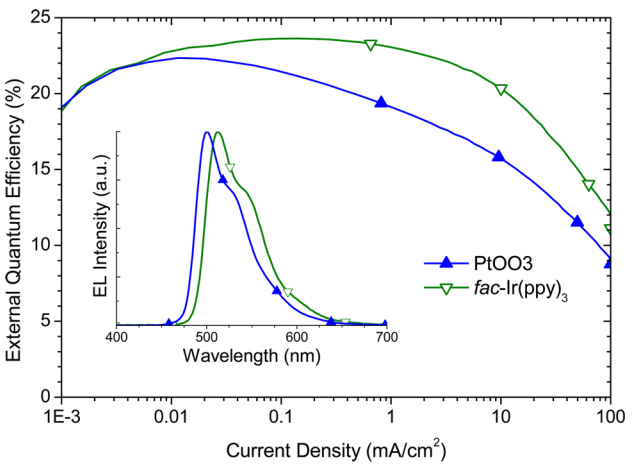

Figure 9. Quantum efficiency-current density characteristics of PtOO3 and *fac*-Ir(ppy)$_3$ devices with the structure of ITO/PEDOT:PSS/TAPC/26mCPy:emitters(8%)/PO15/BmPyPB/LiF/Al. Inset shows the EL spectra of the PtOO3 and *fac*-Ir(ppy)$_3$ devices.

(EQE) of over 20%, peaking at 22.3% ph/el and 23.6% ph/el for PtOO3 and *fac*-Ir(ppy)$_3$ respectively, which is close to the theoretical limit of device efficiency for an OLED on a planar glass substrate.[16] Despite their similar current−voltage (I−V) characteristics (Supporting Information, Figure S3), at high currents the EQE of the device employing PtOO3 begins to drop off more rapidly than that of the *fac*-Ir(ppy)$_3$. This can be

dx.doi.org/10.1021/ic302490c | Inorg. Chem. XXXX, XXX, XXX−XXX

attributed to charge imbalance within the emissive layer at high currents.[28] Nevertheless, PtOO3 devices were still able to demonstrate remarkably high quantum efficiencies at practical emission intensities of 20.6% ph/el at 100 cd/m^2 and 17.6% ph/el at 1000 cd/m^2.

CONCLUSION

On the basis of a novel molecular engineering method, a series of efficient platinum complexes of the type Pt[N^\C−O−LL′] were synthesized, including PtOO3, a cyclometalated platinum complex with an emission quantum yield close to unity. When incorporated into an OLED device, it achieved approximately 100% electron-to-photon conversion efficiency. A similar influence of the popy ligand on the excited state was observed for the deep-blue emitting complex PtOO1 and the blue-green emitting complex PtOO2, which both demonstrated emission quantum efficiencies of over 0.80 (Table 1). This method could be used to develop more efficient phosphorescent complexes, including those in the blue region where there is currently a deficiency. Progress in this area is vital to the continued development of OLED technology for full-color display and solid state lighting applications. It is worth mentioning that the popy ligand will not be the only candidate for LL′ ligands in such a study. More work needs to be completed in order to uncover the relationship between the structure and the photophysical properties of platinum complexes. Moreover, the method of controlling the excited state properties with ancillary ligands can be expanded to different metal systems, continuing to enrich the understanding of the photophysics of luminescent metal complexes.

EXPERIMENTAL SECTION

X-Ray Crystallography. X-ray diffraction data were collected on a Bruker SMART APEX CCD diffractometer with graphite-monochromated Mo Kα radiation (λ = 0.71073 Å) at 296.0(2) K for PtOO1. A sphere of diffraction data was collected up to a resolution of 0.84 Å, and the intensity data were processed using the SAINT program. The cell parameters for the platinum complexes were obtained from the least-squares refinement of spots (from 1818 collected frames for each compound) using the SAINT program. Absorption corrections were applied by using SADABS.[47] All calculations for the structure determination were carried out using the SHELXTL package (version 6.14).[48] Initial platinum atomic positions were located by Patterson methods using XS, and the remaining structure of PtOO1 was found using difference maps and refined by least-squares methods using SHELXL-97 with 2112 independent reflections within the range of θ = 2.61−24.92° (completeness 100.0%). Calculated hydrogen positions were input and refined in a riding manner along with the attached carbons. A summary of the refinement details and resulting factors is given in the Supporting Information (Table S1).

Photophysical Measurements. The UV−visible spectra were recorded on a Hewlett-Packard 4853 diode array spectrometer. Steady state emission experiments at room temperature were performed on a Horiba Jobin Yvon FluoroLog-3 spectrometer. Solution quantum efficiency measurements were carried out at room temperature in a solution of dichloromethane. Before emission spectra were measured, the solutions were thoroughly bubbled with nitrogen inside of a glovebox with an oxygen content less than 1 ppm. Solutions of coumarin 47 (coumarin 1, Φ = 0.73)[49] in ethanol were used as a reference. The equation $\Phi_s = \Phi_r((\eta_s^2 A_r I_s)/(\eta_r^2 A_s I_r))$ was used to calculate the quantum yields. The subscript s denotes the sample, subscript r the coumarin reference, Φ the quantum yield, η the refractive index, A the absorbance, and I the integrated area of the emission band.[50] Phosphorescence lifetime measurements were performed on the same spectrometer with a time correlated single photon counting method using a LED excitation source. The absolute PL quantum efficiency measurements of doped thin film were carried out on a Hamamatsu C9920 system equipped with a xenon lamp, integrating sphere, and a model C10027 photonic multichannel analyzer. PL transient measurements of doped thin films were carried out using the time correlated single photon counting method using a Horiba Jobin Yvon Fluorolog-3 integrated with an IBH Datastation Hub using a 370 nm NanoLED as the excitation source while the sample compartment was purged thoroughly in nitrogen.

Material Identification. Elemental analysis was performed at the Shanghai Institute of Organic Chemistry. NMR spectra were recorded on a Varian Gemini-400 instrument, and chemical shifts were referenced to residual protiated solvent.

Density Functional Theory. Density functional theory (DFT) calculations were performed using the Titan software package (Wave function, Inc.) at the B3LYP/LACVP** level.[22,51,52] The HOMO and LUMO energies were determined using a minimized singlet geometry to approximate the ground state.

Electrochemistry. Cyclic voltammetry and differential pulsed voltammetry were performed using a CH Instrument 610B electrochemical analyzer. Anhydrous dimethylformamide was used as the solvent under a nitrogen atmosphere, and 0.1 M tetra-*n*-butylammonium hexafluorophosphate was used as the supporting electrolyte. A silver wire was used as the pseudo-reference electrode. A platinum wire was used as the counter electrode, and glassy carbon was used as the working electrode. The redox potentials are based on the values measured from differential pulsed voltammetry and are reported relative to a ferrocenium/ferrocene (Fc^+/Fc) redox couple used as an internal reference (0.45 V vs SCE).[53] The reversibility of reduction or oxidation was determined using cyclic voltammetry.[54] As defined, if the magnitude of the peak anodic and the peak cathodic currents have an equal magnitude at scan speeds of 100 mV/s or slower, then the process is considered reversible; if the magnitude of the peak anodic and the peak cathodic currents are not equal, but the return sweeps are nonzero, the process is considered quasi-reversible; otherwise, the process is considered irreversible.

Synthesis. Tetradentate ligands and comparative platinum compounds were prepared using literature methods from commercially available starting materials which were used without further purification. A summary of the procedures employed for ligand synthesis is available in the Supporting Information.

PtOO1. A mixture of 2-(3-(3-(3,5-dimethyl-1H-pyrazol-1-yl)-phenoxy)phenoxy)pyridine (0.34 g, 0.001 mol), K_2PtCl_4 (0.41 g, 0.001 mol), and acetic acid (35 mL) was refluxed under nitrogen for 3 days. After the solvent was removed under vacuum conditions, a dichloromethane solution was added to the solid. Then the solution was filtered, and the filtrate was rotary evaporated to dryness. The oily raw product was then flash chromatographed on a silica column using dichloromethane and isolated with a 45% yield. The raw product was further purified by recrystallization through slow diffusion of ether into dichloromethane followed by thermal evaporation. Anal. Calcd. for $C_{22}H_{17}N_3O_2Pt$: C, 48.00%; H, 3.11%; N, 7.63%. Found: C, 48.06%; H, 3.21%; N, 7.62%. ^{1}H NMR (400 MHz, $CDCl_3$): δ 2.17 (s, 3H), 2.66 (s, 3H), 6.03 (s, 1H), 6.88−7.01 (m, 3H), 7.04−7.12 (m, 3H), 7.17 (vt, 1H, *J* 7.8 Hz), 7.32 (d, 1H, *J* 8.3 Hz), 7.83 (ddd, 1H, *J* 8.5, 7.1, 1.7 Hz), 8.78 (dd, 1H, *J* 5.9, 1.7 Hz). ^{13}C NMR (d_6-DMSO): 14.45 (1C), 14.58 (1C), 105.89 (1C), 107.90 (1C), 110.49 (1C), 110.66 (1C), 112.24 (1C), 112.59 (1C), 112.70 (1C), 116.09 (1C), 120.54, (1C), 124.57 (1C), 125.24 (1C), 142.00 (1C), 142.53 (1C), 147.57 (1C),150.33 (1C), 152.31 (1C), 152.43 (1C), 153.45 (1C), 155.81 (1C), 159.80 (1C).

PtOO2. The complex was prepared in a synthetic procedure similar to PtOO1 with a 50% yield. Anal. Calcd. for $C_{21}H_{15}N_3O_2Pt$: C, 47.02%; H, 2.82%; N, 7.83%. Found: C, 47.00%; H, 2.94%; N, 7.77%. ^{1}H NMR (400 MHz, $CDCl_3$): δ 4.02 (s, 3H), 6.91 (dd, 1H, *J* 7.2, 1.7 Hz), 6.93 (d, 1H, *J* 1.2 Hz), 7.01 (d, 1H, *J* 1.4 Hz), 7.04−7.13 (m, 4H), 7.17 (vt, 1H, *J* 8.1 Hz), 7.27 (dd, 1H, *J* 7.1, 1.0 Hz), 7.32 (d, 1H, *J* 8.2 Hz), 7.90 (ddd, 1H, *J* 8.4, 7.1, 1.8 Hz), 8.81 (dd, 1H, *J* 5.9, 1.6 Hz). ^{13}C NMR ($CDCl_3$): 35.87 (1C), 104.00 (1C), 109.85(1C), 112.83 (1C), 116.26 (1C), 117.22 (1C), 117.37 (1C), 119.16 (1C), 122.16 (1C), 122.64 (1C), 124.23 (1C), 124.44 (1C), 124.50 (1C),

dx.doi.org/10.1021/ic302490c | Inorg. Chem. XXXX, XXX, XXX−XXX

137.85 (1C), 139.82 (1C), 149.00 (1C), 152.84 (1C), 154.54 (1C), 155.07 (1C), 159.55 (1C).

PtOO3. The complex was prepared in a synthetic procedure similar to PtOO1 with a 70% yield. Anal. Calcd. for $C_{22}H_{14}N_2O_2Pt$: C, 49.53%; H, 2.65%; N, 5.25%. Found: C, 49.57%; H, 2.78%; N, 5.19%. ^{1}H NMR (400 MHz, $CDCl_3$): δ 6.95 (dd, 1H, J 7.2, 1.8 Hz), 7.12−7.27 (m, 6H), 7.33 (d, 1H, J 8.3 Hz), 7.50 (dd, 1H, J 7.2, 1.4 Hz), 7.82 (ddd, 1H, J 8.6, 7.2, 1.6 Hz), 7.88 (ddd, 1H, J 8.7, 7.1, 1.9 Hz), 7.92 (d, 1H, J 8.1 Hz), 8.30 (d, 1H, J 5.5 Hz), 8.48 (dd, 1H, J 5.7, 1.9 Hz). ^{13}C NMR (d_6-DMSO): 106.24 (1C), 110.25 (1C), 112.69 (1C), 116.11 (1C), 117.38 (1C), 119.31 (1C), 120.46 (1C), 122.00 (1C), 124.23 (1C), 124.82 (1C), 124.89, (1C), 125.72 (1C), 139.44 (1C), 142.20 (1C), 147.66 (1C), 148.69 (1C), 149.46 (1C), 152.06 (1C), 154.01 (1C), 155.99 (1C), 159.82 (1C), 164.44 (1C).

OLED Fabrication and Testing. Devices employing PtOO3 and *fac*-Ir(ppy)$_3$ as emitters were fabricated on glass substrates precoated with a patterned transparent indium tin oxide (ITO) anode using a device architecture of ITO/PEDOT:PSS/20 nm TAPC/25 nm 8% emitter:26mCPy/10 nm PO15/30 nm BmPyPB/LiF/Al, where PEDOT:PSS = poly(3,4-ethylenedioxythiophene) poly-(styrenesulfonate), TAPC[55] = 1,1-bis[4-[N,N′-di(p-tolyl)amino]-phenyl] cyclohexane, 26mCPy[11] = 2,6-bis(N-carbazolyl)pyridine, PO15[56] = 2,8-bis(diphenylphosphoryl)-dibenzothiophene, and BmPyPB[57] = 1, 3-bis[3, 5-di(pyridin-3-yl)phenyl]benzene).

Prior to organic depositions, the ITO substrates were cleaned by subsequent sonication in water, acetone, and isopropanol followed by a 15 min UV−ozone treatment. PEDOT:PSS was filtered through a 0.2 μm filter and spin-coated on the prepared substrates, giving a 40-nm-thick film. All small molecular organic materials were deposited by thermal evaporation at rates of 0.5 to 1.5 Å/s with a working pressure of less than 10^{-7} Torr. A thin 1 nm LiF layer was deposited at a rate of <0.2 Å/s and aluminum cathodes were deposited at 1−2 Å/s through a shadow mask without breaking the vacuum. Individual devices have areas of 0.04 cm^2. I−V−L characteristics were taken with a Keithley 2400 Source-Meter and a Newport 818 Si photodiode inside a nitrogen-filled glovebox. Electroluminescence (EL) spectra were taken using the Jobin Yvon Fluorolog spectrofluorometer. Agreement between luminance, optical power, and EL spectra was verified with a calibrated Photo Research PR-670 spectroradiometer with all devices assumed to be Lambertian emitters.

■ ASSOCIATED CONTENT

Ⓢ Supporting Information

X-ray crystallographic data for PtOO1 in CIF format. Synthesis and ^{1}H NMR characterization of the ligands. Cyclic voltammetry scans of PtOO1, PtOO2, and PtOO3. Current−voltage plot of PtOO3 and *fac*-Ir(ppy)$_3$ OLED devices. ^{1}H NMR spectra and assignment of complexes. This material is available free of charge via the Internet at http://pubs.acs.org.

■ AUTHOR INFORMATION

Corresponding Author

*E-mail: Jian.Li.1@asu.edu.

Author Contributions

The manuscript was written through contributions of all authors. All authors have given approval to the final version of the manuscript.

Notes

The authors declare no competing financial interest.

■ ACKNOWLEDGMENTS

The authors thank Jason Brooks from Universal Display Corporation for thin film quantum efficiency measurements, Professor Jinbo Hu of the Shanghai Institute of Organic Chemistry for EA and discussion, and Thomas Groy of ASU for XRD measurements. Financial support was provided by NSF (CHE-0748867).

■ REFERENCES

(1) Wu, W.; Xu, X.; Yang, H.; Hua, J.; Zhang, X.; Zhang, L.; Long, Y.; Tian, H. *J. Mater. Chem.* **2011**, *21*, 10666−10671.

(2) Demas, J. N.; Harris, E. W.; Flynn, C. M.; Diemente, D. *J. Am. Chem. Soc.* **1975**, *97*, 3838−3839.

(3) Gao, R.; Ho, D. G.; Hernandez, B.; Selke, M.; Murphy, D.; Djurovich, P. I.; Thompson, M. E. *J. Am. Chem. Soc.* **2002**, *124*, 14828−14829.

(4) Zhang, D.; Wu, L.; Zhou, L.; Han, X.; Yang, Q.; Zhang, L.; Tung, C. *J. Am. Chem. Soc.* **2004**, *126*, 3440−3441.

(5) Feng, K.; Zhang, R.; Wu, L.; Tu, B.; Peng, M.; Zhang, L.; Zhao, D.; Tung, C. *J. Am. Chem. Soc.* **2006**, *128*, 14685−14690.

(6) Kunugi, Y.; Mann, K. R.; Miller, L. L.; Exstrom, C. L. *J. Am. Chem. Soc.* **1998**, *120*, 589−590.

(7) Thomas, S. W., III; Venkatesan, K.; Mueller, P.; Swager, T. M. *J. Am. Chem. Soc.* **2006**, *128*, 16641−16648.

(8) Siu, P. K. M.; Lai, S.; Lu, W.; Zhu, N.; Che, C. *Eur. J. Inorg. Chem.* **2003**, 2749−2752.

(9) Baldo, M. A.; O'Brien, D. F.; You, Y.; Shoustikov, A.; Sibley, S.; Thompson, M. E.; Forrest, S. R. *Nature* **1998**, *395*, 151−154.

(10) Baldo, M. A.; Lamansky, S.; Burrows, P. E.; Thompson, M. E.; Forrest, S. R. *Appl. Phys. Lett.* **1999**, *75*, 4−6.

(11) Williams, E.; Haavisto, K.; Li, J.; Jabbour, G. *Adv. Mater.* **2007**, *19*, 197−202.

(12) Yang, X.; Wang, Z.; Madakuni, S.; Li, J.; Jabbour, G. E. *Adv. Mater.* **2008**, *20*, 2405−2409.

(13) Sotoyama, W.; Satoh, T.; Sawatari, N.; Inoue, H. *Appl. Phys. Lett.* **2005**, *86*, 153505.

(14) Lu, W.; Chan, M. C. W.; Zhu, N.; Che, C.; Li, C.; Hui, Z. *J. Am. Chem. Soc.* **2004**, *126*, 7639−7651.

(15) Sommer, J. R.; Farley, R. T.; Graham, K. R.; Yang, Y.; Reynolds, J. R.; Xue, J.; Schanze, K. S. *ACS Appl. Mater. Interfaces* **2009**, *1*, 274−278.

(16) Adachi, C.; Baldo, M. A.; Thompson, M. E.; Forrest, S. R. *J. Appl. Phys.* **2001**, *90*, 5048−5051.

(17) Kawamura, Y.; Goushi, K.; Brooks, J.; Brown, J. J.; Sasabe, H.; Adachi, C. *Appl. Phys. Lett.* **2005**, *86*, 071104.

(18) Sajoto, T.; Djurovich, P. I.; Tamayo, A. B.; Oxgaard, J.; Goddard, W. A.; Thompson, M. E. *J. Am. Chem. Soc.* **2009**, *131*, 9813−9822.

(19) Williams, J. A. G.; Develay, S.; Rochester, D.; Murphy, L. *Coord. Chem. Rev.* **2008**, *252*, 2596−2611.

(20) Yersin, H.; Rausch, A.; Czerwieniec, R.; Hofbeck, T.; Fischer, T. *Coord. Chem. Rev.* **2011**, *255*, 2622−2652.

(21) Yersin, H. *Top. Curr. Chem.* **2004**, *241*, 1−26.

(22) Brooks, J.; Babayan, Y.; Lamansky, S.; Djurovich, P. I.; Tsyba, I.; Bau, R.; Thompson, M. E. *Inorg. Chem.* **2002**, *41*, 3055−3066.

(23) Chassot, L.; Von Zelewsky, A. *Inorg. Chem.* **1987**, *26*, 2814−2818.

(24) Williams, J. A. G.; Beeby, A.; Davies, E. S.; Weinstein, J. A.; Wilson, C. *Inorg. Chem.* **2003**, *42*, 8609−8611.

(25) Wang, Z.; Turner, E.; Mahoney, V.; Madakuni, S.; Groy, T.; Li, J. *Inorg. Chem.* **2010**, *49*, 11276−11286.

(26) Rausch, A. F.; Murphy, L.; Williams, J. A. G.; Yersin, H. *Inorg. Chem.* **2009**, *48*, 11407−11414.

(27) Ravindranathan, D.; Vezzu, D. A. K.; Bartolotti, L.; Boyle, P. D.; Huo, S. *Inorg. Chem.* **2010**, *49*, 8922−8928.

(28) Willison, S. A.; Krause, J. A.; Connick, W. B. *Inorg. Chem.* **2008**, *47*, 1258−1260.

(29) Fleetham, T.; Wang, Z.; Li, J. *Org. Electron.* **2012**, *13*, 1430−1435.

(30) Rausch, A.; Murphy, L.; Williams, J. A. G.; Yersin, H. *Inorg. Chem.* **2012**, *51*, 312−319.

(31) Kui, S.; Chow, P. K.; Tong, G. S. M.; Lai, S.; Cheng, G.; Kwok, C.; Low, K.; Ko, M. Y.; Che, C. *Chem.—Eur. J.* **2013**, *19*, 69−73.

(32) Che, C.; Kwok, C.; Lai, S.; Rausch, A.; Finkenzeller, W.; Zhu, N.; Yersin, H. *Chem.—Eur. J.* **2010**, *16*, 233−247.
(33) Lin, Y.; Chan, S.; Chan, M. C. W.; Hou, Y.; Zhu, N.; Che, C.; Liu, Y.; Wang, Y. *Chem.—Eur. J.* **2003**, *9*, 1263−1272.
(34) Vezzu, D. A. K.; Deaton, J. C.; Jones, J. S.; Bartolotti, L.; Harris, C. F.; Marchetti, A. P.; Kondakova, M.; Pike, R. D.; Huo, S. *Inorg. Chem.* **2010**, *49*, 5107−5119.
(35) Feng, K.; Zuniga, C.; Zhang, Y.; Kim, D.; Barlow, S.; Marder, S. R.; Brédas, J. L.; Weck, M. *Macromolecules* **2009**, *42*, 6855−6864.
(36) Huo, S.; Harris, C. F.; Vezzu, D. A. K.; Gagnier, J. P.; Smith, M. E.; Pike, R. D.; Li, Y. *Polyhedron* **2012**, DOI: 10.1016/j.poly.2012.06.078.
(37) Evans, R. C.; Douglas, P.; Winscom, C. J. *Coord. Chem. Rev.* **2006**, *250*, 2093−2126.
(38) Li, J.; Djurovich, P. I.; Alleyne, B. D.; Yousufuddin, M.; Ho, N. N.; Thomas, J. C.; Peters, J. C.; Bau, R.; Thompson, M. E. *Inorg. Chem.* **2005**, *44*, 1713−1727.
(39) Chou, P. T.; Chi, Y.; Chung, M. W.; Lin, C. C. *Coord. Chem. Rev.* **2011**, *255*, 2653−2665.
(40) Schareina, T.; Zapf, A.; Cotté, A.; Müller, N.; Beller, M. *Tetrahedron Lett.* **2008**, *49*, 1851−1855.
(41) Wang, Z.; Bao, W.; Jiang, Y. *Chem. Commun.* **2005**, *0*, 2849−2851.
(42) Bellina, F.; Cauteruccio, S.; Rossi, R. *Chem.—Eur. J.* **2006**, *2006*, 1379−1382.
(43) Littke, A. F.; Schwarz, L.; Fu, G. C. *J. Am. Chem. Soc.* **2002**, *124*, 6343−6348.
(44) Develay, S.; Blackburn, O.; Thompson, A. L.; Williams, J. G. *Inorg. Chem.* **2008**, *47*, 11129−11142.
(45) Kvam, P.; Puzyk, M. V.; Balashev, K. P.; Songstad, J. *J. Acta Chem. Scand.* **1995**, *49*, 335−343.
(46) Cummings, S. D.; Eisenberg, R. *J. Am. Chem. Soc.* **1996**, *118*, 1949−1960.
(47) Blessing, R. H. *Acta Crystallogr.* **1995**, *51*, 33−38.
(48) Sheldrick, G. M. *Acta Crystallogr.* **2003**, *A64*, 112−122.
(49) Jones, G.; Jackson, W. R.; Choi, C. Y.; Bergmark, W. R. *J. Phys. Chem.* **1985**, *89*, 294−300.
(50) DePriest, J.; Zheng, G. Y.; Goswami, N.; Eichhorn, D. M.; Woods, C.; Rillema, D. P. *Inorg. Chem.* **2000**, *39*, 1955−1963.
(51) Hay, P. J. *J. Phys. Chem. A* **2002**, *106*, 1634−1641.
(52) Tamayo, A. B.; Alleyne, B. D.; Djurovich, P. I.; Lamansky, S.; Tsyba, I.; Ho, N. N.; Bau, R.; Thompson, M. E. *J. Am. Chem. Soc.* **2003**, *125*, 7377−7387.
(53) Connelly, N. G.; Geiger, W. E. *Chem. Rev.* **1996**, *96*, 877−910.
(54) Harris, D. C. In *Quantitative Chemical Analysis, Sixth ed.*; W. H. Freeman: New York, 2002; pp 394−396.
(55) Sasabe, H.; Gonmori, E.; Chiba, T.; Li, Y.; Tanaka, D.; Su, S.; Takeda, T.; Pu, Y.; Nakayama, K.; Kido, J. *Chem. Mater.* **2008**, *20*, 5951−5953.
(56) Cai, X.; Padmaperuma, A. B.; Sapochak, L. S.; Vecchi, P. A.; Burrows, P. E. *Appl. Phys. Lett.* **2008**, *92*, 083308−083308−3.
(57) Su, S.; Gonmori, E.; Sasabe, H.; Kido, J. *Adv. Mater.* **2008**, *20*, 4189−4194.